

Cite this: *Chem. Sci.*, 2022, 13, 6744

All publication charges for this article have been paid for by the Royal Society of Chemistry

Received 26th March 2022

Accepted 15th May 2022

DOI: 10.1039/d2sc01748b

rsc.li/chemical-science

Synthesis and characterisation of the ternary intermetalloid clusters $\{M@[As_8(ZnMes)_4]\}^{3-}$ ($M = Nb, Ta$) from binary $[M@As_8]^{3-}$ precursors†

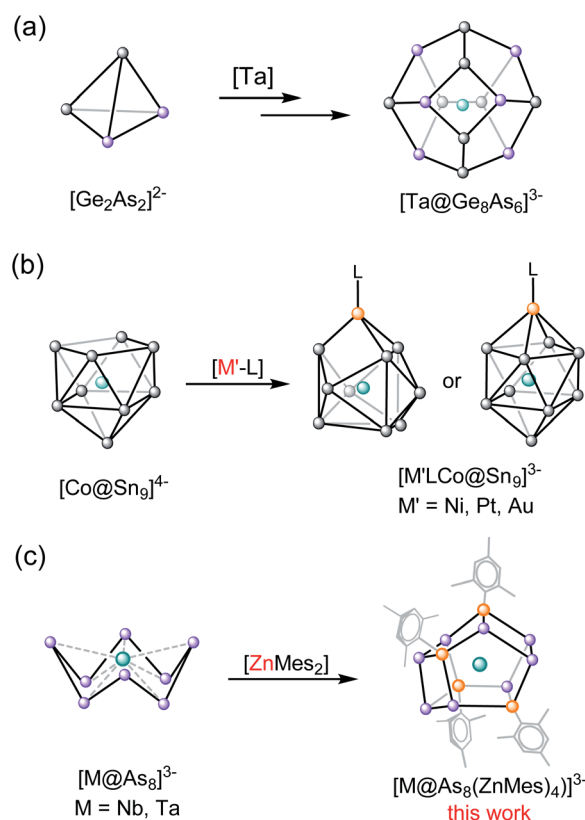
Wei-Qiang Zhang,^a Harry W. T. Morgan,^b John E. McGrady^b and Zhong-Ming Sun^{a*}

The development of rational synthetic routes to inorganic arsenide compounds is an important goal because these materials are finding applications in many areas of materials science. In this paper, we show that the binary crown clusters $[M@As_8]^{3-}$ ($M = Nb, Ta$) can be used as synthetic precursors which, when combined with $ZnMes_2$, generate ternary intermetalloid clusters with 12-vertex cages, $\{M@[As_8(ZnMes)_4]\}^{3-}$ ($M = Nb, Ta$). Structural studies are complemented by mass spectrometry and an analysis of the electronic structure using DFT. The synthesis of these clusters presents new opportunities for the construction of As-based nanomaterials.

Introduction

Ternary intermetalloid clusters have attracted a great deal of attention in the recent literature due to their complex electronic structures and also their potential role in materials science.^{1–3} The majority of known clusters in this class are synthesised either by extraction of the corresponding quaternary intermetallic phases or by the reaction of binary Tt/Pn or Tr/Pn Zintl anions with sources of low-valent transition metals, lanthanides or actinides.^{4–6} Scheme 1a illustrates the extraction of the quaternary solid-state Zintl phase $K/Ge/As/M$ ($M = V, Nb, Ta$) in ethylenediamine (en) in the presence of the sequestering agent, [2.2.2]crypt, which allows for the crystallization of cluster anions including 12-vertex $[M@Ge_8As_4]^{3-}$ ($M = V, Ta$), and 14-vertex $[M@Ge_8As_6]^{3-}$ ($M = Nb, Ta$).^{7,8} Clusters such as $[Zn@Zn_5Sn_3Bi_3@Bi_5]^{4-}$,⁹ $[Ni_2@Sn_7Bi_5]^{3-}$,¹⁰ $[Pd_3@Sn_8Bi_6]^{4-}$,¹¹ $[Pd@Pd_2Pb_{10}Bi_6]^{4-}$,¹² and $[Eu@Sn_6Bi_8]^{4-}$,¹³ have, in contrast, been accessed by reacting a salt of a binary mixed main group Zintl compound, $[K([2.2.2]crypt)]_2[TrBi_3] \cdot en$ ($Tr = Ga, In, Tl$) or $[K([2.2.2]crypt)]_2[Tt_2Pn_2] \cdot en$ ($Tt/Pn = Sn/Sb, Sn/Bi, Pb/Bi$)^{14,15} with various organometallic compounds. A variant on this approach is to use a preformed binary intermetalloid where the central transition metal is already in place, surrounded by a shell of main-group atoms, as a starting material to react with

other transition metal salts (Scheme 1b). This protocol has been used, for example, in the synthesis of $[(L)MCo@Sn_9]^{3-}$ from the reaction of $[Co@Sn_9]^{4-}$, extracted from the ternary phase



Scheme 1 (a and b) Selected examples of ternary intermetalloid cluster anions of the general formula $[M_m@E_x^{1E_y^2}]^{q-}$ synthesised by different methods. (c) This work.

^aState Key Laboratory of Elemento-Organic Chemistry, Tianjin Key Lab of Rare Earth Materials and Applications, School of Materials Science and Engineering, Nankai University, Tianjin 300350, China. E-mail: sunlab@nankai.edu.cn

^bDepartment of Chemistry, University of Oxford, South Parks Road, Oxford, OX1 3QR, UK. E-mail: john.mcgrady@chem.ox.ac.uk

† Electronic supplementary information (ESI) available: Full experimental, computational details and ESI-MS spectra. CCDC 2078235 (1), 2093790 (2). For ESI and crystallographic data in CIF or other electronic format see <https://doi.org/10.1039/d2sc01748b>

"K₅Co₃Sn₉", with group 10-containing precursors such as [Ni(CO)₂(PPh₃)₂], [Ni(cod)₂], [Pt(PPh₃)₄] or [Au(PPh₃)Ph].¹⁶ It is significant that these reactions involve only a simple ligand exchange reaction, and do not cause a substantial rearrangement of the binary inter-metalloid cluster core.¹⁷

The extension of this protocol to clusters containing group 15 elements has not been explored in detail, but there is a readily accessible family of starting materials available in the form of the crown-like [M@As₈]^{3−} clusters, the first example of which, [Nb@As₈]^{3−}, was reported in 1986.¹⁸ Since then, the family has been extended to include [Mo@As₈]^{2−},¹⁹ and [Cr@As₈]^{3−},²⁰ as well as the Sb analogues, [Mo@Sb₈]^{3−} and [Nb@Sb₈]^{3−}.^{20,21} A broad survey of the electronic structure of the [M@Pn₈]^{n−} family, encompassing M = Cr, Mo, Mn, Tc, Re, Ti, Zr, Hf and Pn = As, Sb; n = 1, 2, 3, has also been reported using density functional theory.²² The four As atoms on either side of the crown in the [M@As₈]^{n−} unit form a region of high electron density, which has the potential to coordinate large alkali metals such as Rb, K, and hence form chain structures such as [∞][RbNbAs₈]^{2−} and [∞][KCrAs₈]^{2−}. In addition, the high oxidation state transition metal ion can serve as a 2-electron acceptor to form d² complexes with Lewis basic reagents.^{1a,22} In a very recent study we showed that the reaction of [M@As₈]^{3−}, M = Nb, Ta, with a source of low-valent Cu can lead to the formation of an extended [As₁₆]^{10−} ligand, where a tri-cyclo As₇ unit is connected to a conserved As₈ crown *via* a bridging As atom.²³ Although mechanistic details are hard to elucidate, this reaction necessarily involves extensive cleavage and rearrangement of As–As bonds. In this paper we extend these studies to report the reactions of [K([2.2.2]crypt)]₃[Nb@As₈] or [K([2.2.2]crypt)]₂[KTa@As₈] with an organometallic source of Zn(II), ZnMes₂. In both cases the reactions generate 12-vertex cage type ternary intermetalloid clusters compounds, [K([2.2.2]crypt)]₃{Nb@[As₈(ZnMes)₄]}·2en·tol (**1**) and [K([2.2.2]crypt)]₃{Ta@[As₈(ZnMes)₄]}·en (**2**) where the As₈^{8−} crown has been split into two As₄^{6−} units, bridged by [ZnMes] fragments. The products are characterised by X-ray crystallography and mass spectrometry, and the electronic structures and formation pathways are explored using density functional theory.

Results and discussion

At elevated temperatures, ethylenediamine (en) solutions of [K([2.2.2]crypt)]₃[Nb@As₈] or [K([2.2.2]crypt)]₂[KTa@As₈] react with a toluene (tol) solution of ZnMes₂ (Mes = 1,3,5-trimethylbenzene) to form [K([2.2.2]crypt)]₃{Nb@[As₈(ZnMes)₄]}·2en·tol (**1**) or [K([2.2.2]crypt)]₃{Ta@[As₈(ZnMes)₄]}·en (**2**), in *ca.* 30% and 25% yield, respectively. In the case of [K([2.2.2]crypt)]₂[KTa@As₈], one further equivalent of [2.2.2]crypt was added to the reaction to sequester the non-encrypted K⁺ ion. Diffusion of the reaction solution afforded dark-green block-like crystals of **1** and red-brown strip-like crystals of **2**, both of which proved suitable for single-crystal X-ray diffraction study. Under similar reaction conditions, [K([2.2.2]crypt)]₃{Ta@[As₈(CdMes)₄]} could also be isolated by replacing ZnMes₂ with CdMes₂ as starting reagent, but we have not yet been able to isolate crystals of sufficient quality to allow full structural

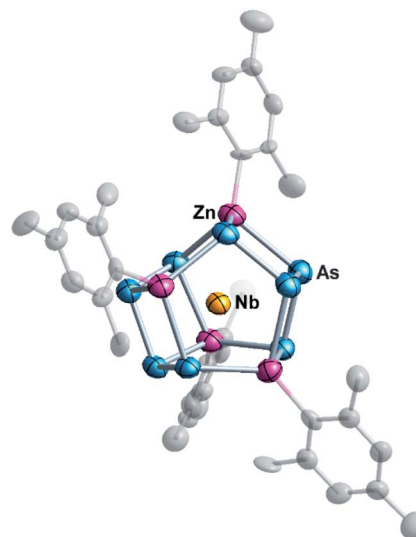


Fig. 1 Molecular structure of the cluster {Nb@[As₈(ZnMes)₄]}^{3−} (**1a**) with thermal ellipsoids at the 50% probability level. The hydrogen atoms are omitted for clarity.

characterization. Both **1** and **2** crystallise in the monoclinic space group *P*2₁/*n* with a single {M@[As₈(ZnMes)₄]}^{3−} (M = Nb, Ta) anion and solvent molecules (en, tol) as well as three [K([2.2.2]crypt)]⁺ cations in the corresponding unit cell. Fig. 1 shows the molecular structure of the cluster anion in **1**: full crystallographic details are given in ESI (Table S1†). For better visualization, different labels are used to distinguish the anionic cluster and the molecular compounds, and **1a–2a** represent the anionic clusters in compounds **1–2**, respectively.

The two anionic clusters {Nb@[As₈(ZnMes)₄]}^{3−} (**1a**) and {Ta@[As₈(ZnMes)₄]}^{3−} (**2a**) are isostructural and adopt almost perfect S₄ point symmetry. They contain two tetrameric zig-zag [As₄]^{6−} oligomers linked by four [ZnMes] groups in a μ₃η^{1:1:1:1} coordination mode. The As–As bond lengths in **1a** and **2a** lie in the range 2.377–2.539 Å, values which are typical of As–As single bonds in polyarsenide Zintl clusters such as As₇^{3−} and As₁₁^{3−}.²⁴ The As–Zn distances (2.497(6)–2.693(6) Å for **1a**, 2.500(9)–2.690(8) Å for **2a**, respectively) are relatively widely dispersed because the As₄^{6−} units contain As centres that are formally mono- and dianionic (in the centre and the termini of the As₄ chains, respectively).²⁵ For comparison, As–Zn bond lengths in [ZnAs₁₅]^{3−} and [ZnAs₁₄]^{4−} are at the shorter end of this range (2.488–2.536 Å,²⁶ and 2.481–2.573 Å,²⁷ respectively). The M–Zn (M = Nb, Ta) distances (2.778(9)–2.796(9) Å for **1a**, 2.782(7)–2.795(8) Å for **2a**) are considerably longer than those in organometallic compounds such as [(C₅H₅)₂NbH₂ZnC₅H₅] (2.541 Å)²⁸ and [(CH₃C₅H₄)₂TaH(ZnC₅H₅)₂] (2.589 Å)²⁹ that are known to contain Nb/Ta–Zn bonds, precluding any direct metal–metal bonding in these clusters.

The overall stoichiometry of the reaction, [M@As₈]^{3−} + 4 'ZnMes' → [M@As₈(ZnMes)₄]^{3−}, suggests a possible mechanistic pathway involving transient [Zn(II)Mes] fragments which cause the reductive cleavage of the As₈^{8−} crown to form the two separate As₄^{6−} fragments present in the product. Power and co-workers have reported a stable dimer of Zn(II)Ar (Ar = C₆H₃-2,6-



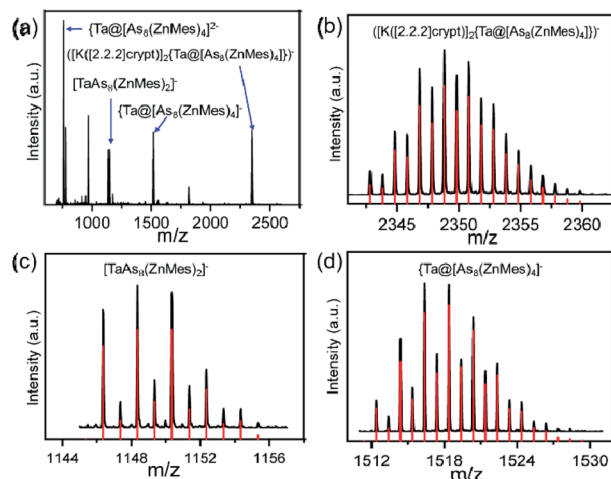


Fig. 2 (a) Negative-ion ESI mass spectrum over the range of m/z 600–3000 of **2**; (b–d) mass spectra of measured and calculated isotope patterns for peak $\{[K([2.2.2]crypt)]_2\{Ta@As_8(ZnMes)_4\}\}^-$ ($m/z = 2348.8193$), $\{TaAs_8(ZnMes)_2\}^-$ ($m/z = 1148.3488$) and $\{Ta@As_8(ZnMes)_4\}^-$ ($m/z = 1518.3754$). The experimental mass distributions are depicted in black, and the theoretical masses of the isotope distribution are shown in red.

$[C_6H_3-2,6-(iPr)_2]$ produced by the reduction of $ArZnCl$ with Na in ethanol,³⁰ but there is no equivalent reducing agent present in these reactions, and the precise mechanism by which the low-valent Zn entities are formed remains uncertain. Reductive elimination of Mes_2 from $ZnMes_2$ is one possibility, and there is literature precedent for similar reactions,³¹ but we have not been able to confirm the presence of Mes_2 in solution. The need for four equivalents of $ZnMes$ to cleave two As–As bonds in the product suggests a stepwise pathway, and indeed we find evidence to support this in the negative-ion mass spectrum of **2** (Fig. 2), which shows prominent peaks for the parent ion at $m/z = 1518.3754$ ($\{Ta@As_8(ZnMes)_4\}^-$) and at $m/z = 2348.8193$ ($\{[K([2.2.2]crypt)]_2\{Ta@As_8(ZnMes)_4\}\}^-$), but also for the cluster with only two $ZnMes$ units, $\{TaAs_8(ZnMes)_2\}^-$ at $m/z = 1148.3488$. It is striking that all of the major peaks in the ESI-MS retain the 1 : 8 ratio of M to As, a clear indication of the robust nature of the $[M@As_8]$ unit, even under quite harsh reaction conditions.

The DFT-computed potential energy profile (ADF2021,³² PBE functional,³³ triple-zeta polarised basis set – full details given in the ESI†) for the reaction of $[Ta@As_8]^{3-}$ with $ZnMes$ shown in Fig. 3 reveals a cascade from reactants to products, with the $\{Ta@[As_8(ZnMes)_2]\}^{3-}$ cluster ($E_{rel} = -3.71$ eV) clearly intermediate in energy between reactant (0) and product (-9.50 eV). The optimised structure of $\{Ta@[As_8(ZnMes)_2]\}^{3-}$ confirms that only a single As–As bond has been broken in the intermediate, generating a contiguous As_8 chain with a formal -10 charge. The computed energies therefore indicate that the stepwise addition of $ZnMes$ to $[Ta@As_8]^{3-}$ leading to $\{Ta@[As_8(ZnMes)_2]\}^{3-}$ and from there to $\{Ta@[As_8(ZnMes)_4]\}^{3-}$ is a viable mechanism, at least thermodynamically, for cluster formation. We note, however, that the $\{Ta@[As_8(ZnMes)_2]\}^{3-}$ intermediate is unstable with respect to disproportionation into reactants

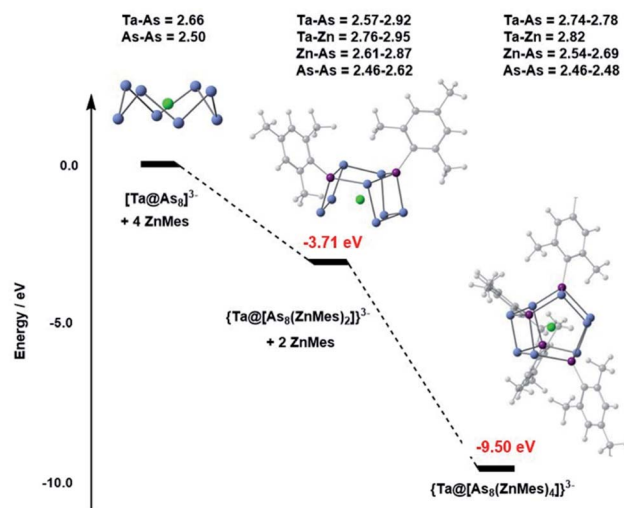


Fig. 3 Potential energy profile for the cascade from $[Ta@As_8]^{3-}$ to $\{Ta@[As_8(ZnMes)_2]\}^{3-}$ and then to $\{Ta@[As_8(ZnMes)_4]\}^{3-}$ (**2a**). The profile for the corresponding reaction with Nb rather than Ta is very similar (relative energies are identical to within 0.05 eV).

and products: $2[Ta@As_8(ZnMes)_2]^{3-} \rightarrow [Ta@As_8]^{3-} + [Ta@[As_8(ZnMes)_4]]^{3-}$, $\Delta E = -2.08$ eV, so is unlikely to be amenable to isolation.

The cluster products obtained from the reaction with $ZnMes_2$ make a striking contrast to the corresponding reactions of $[M@As_8]^{3-}$ with $[CuMes(PPh_3)_2] \cdot tol$ described in our previous paper,²³ where two As_8 units merged to form a single contiguous As_{16} ¹⁰⁻ ligand. The mechanistic details of the reactions with Cu are far from clear, not least because, unlike the reactions described here, the Nb/Ta : As ratio is different in reactants and products. Nevertheless, reductive cleavage of the As_8 crown into As_4 fragments is clearly not involved, and the key difference between the two metal reagents, $ZnMes_2$ here and $[CuMes(PPh_3)_2] \cdot tol$ in the previous work, appears, therefore, to be the greater accessibility of transient monovalent “ $ZnMes$ ” compared to zerovalent Cu.

Comparison to other 12-vertex clusters

A complementary perspective on the bonding in these clusters comes from noting their formal relationship to the $\{M@[Ge_8As_4]\}^{3-}$ ($M = V, Ta$) clusters reported recently by Dehnen and co-workers (Fig. 4).³⁴ The $[ZnMes]^{2-}$ fragment is isolobal with Ge^- and also with As, and so the 60-electron, 12-vertex cages can be formulated as $[Ge_8As_4]^{8-}$ in $\{Ta@[Ge_8As_4]\}^{3-}$ and as $[As_8(ZnMes)_4]^{8-}$ in $\{Ta@[As_8(ZnMes)_4]\}^{3-}$. The projected densities of states (PDOS) for the two Ta-based clusters, $\{Ta@[As_8(ZnMes)_4]\}^{3-}$ and $\{Ta@[Ge_8As_4]\}^{3-}$, are also compared in Fig. 4. The contribution of Ta 5d orbitals to the occupied manifold is minor in both cases, suggesting that the Ta(v) oxidation state is a reasonable first approximation for the electronic structure. In the $\{Ta@[Ge_8As_4]\}^{3-}$ case, there is substantial mixing between the Ge and As 4s/4p manifolds in both the occupied and virtual space, and the peaks that lie ~ 1.0 eV above and below the Fermi level have Ge and As

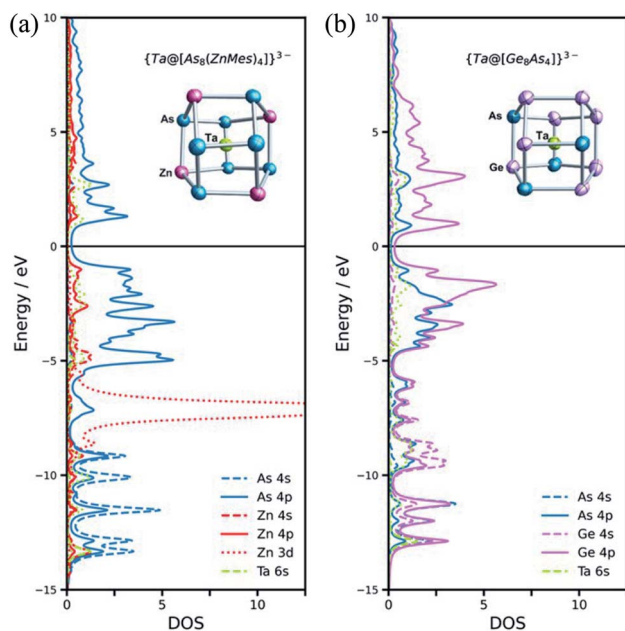


Fig. 4 Structures and projected densities of states for the 12-vertex cluster anions $\{Ta@[As_8(ZnMes)_4]\}^{3-}$ (2a) (a) and $[Ta@Ge_8As_4]^{3-}$ (b), with thermal ellipsoids at the 50% probability level. The molecular structures of $\{Ta@[Ge_8As_4]\}^{3-}$ is disordered, and the calculated minimum structure is presented here. The organic – Mes ligands are omitted in $\{Ta@[As_8(ZnMes)_4]\}^{3-}$. The projected DOS is summed over all atoms of a given type.

character in approximately equal proportion. In contrast, the As 4s/4p and Zn 4s/4p manifolds are well separated, and As 4p character dominates the window 5 eV either side of the Fermi level. Thus, whilst the structural chemistry and the formal valence electron count point to a close relationship between the two clusters, the bonding is significantly more ionic in the Zn/As clusters reported here than in the Ge/As analogues.

Conclusions

In summary, we have established that the $[Nb@As_8]^{3-}$ and $[Ta@As_8]^{3-}$ anions can be used as synthetic precursors to ternary As-rich clusters where the M : As ratio of 1 : 8 is conserved. Their reactions with $ZnMes_2$ yield cluster compounds of the general formula $\{M@[As_8(ZnMes)_4]\}^{3-}$ (M = Nb, Ta), where two As–As bonds of the original crown-like As_8^{8-} unit are cleaved to form two As_4^{6-} fragments. The presence of clusters with two, rather than four, $[ZnMes]$ units in the ESI-MS spectra suggests a step-wise pathway where $[ZnMes]$ units are added sequentially with progressive fragmentation of the As_8 ring. The reaction of $[M@As_8]$ units with low-valent transition metal organometallics described in this paper presents new possibilities for the construction of ternary arsenic-rich nano-clusters with tightly controlled stoichiometries.

Data availability

Detailed experimental procedures, crystallographic supplementation, electrospray ionization mass spectrometry (ESI-MS)

analysis, energy-dispersive X-ray (EDX) spectroscopic analysis, and quantum-chemical studies can be found in the ESI.†

Author contributions

Z. M. S. conceived the project and designed the experiments. W. Q. Z. performed the synthesis and the single-crystal X-ray diffraction as well as analysed the data. H. W. T. M. and J. E. M. performed the quantum chemical calculations and analysed the data. All authors co-wrote the manuscript.

Conflicts of interest

There are no conflicts to declare.

Acknowledgements

This work was supported by the National Natural Science Foundation of China (92161102 and 21971118) and the Natural Science Foundation of Tianjin City (No. 20JCYBJC01560 and B2021202077) as well as the 111 project (B18030) from China. H. W. T. M. thanks the EPSRC for support through the Centre for Doctoral Training, Theory and Modelling in Chemical Sciences under Grant EP/L015722/1.

Notes and references

- (a) R. J. Wilson, N. Lichtenberger, B. Weinert and S. Dehnen, *Chem. Rev.*, 2019, **119**, 8506–8554; (b) S. Scharfe, F. Kraus, S. Stegmaier, A. Schier and T. F. Fässler, *Angew. Chem., Int. Ed.*, 2011, **50**, 3630–3671.
- T. F. Fässler and S. D. Hoffmann, *Angew. Chem., Int. Ed.*, 2004, **43**, 6242–6247.
- J. E. McGrady, F. Weigend and S. Dehnen, *Chem. Soc. Rev.*, 2022, **51**, 628–649.
- (a) N. Lichtenberger, R. J. Wilson, A. R. Eulenstein, W. Massa, R. Clérac, F. Weigend and S. Dehnen, *J. Am. Chem. Soc.*, 2016, **138**, 9033–9036; (b) K. Mayer, J. V. Dums, W. Klein and T. F. Fässler, *Angew. Chem., Int. Ed.*, 2017, **56**, 1–6.
- (a) B. Weinert, F. Weigend and S. Dehnen, *Chem.–Eur. J.*, 2012, **18**, 13589–13595; (b) R. Ababei, W. Massa, B. Weinert, P. Pollak, X. Xie, R. Clérac, F. Weigend and S. Dehnen, *Chem.–Eur. J.*, 2015, **21**, 386–394; (c) F. X. Pan, C. Q. Xu, L. J. Li, X. Min, J. Q. Wang, J. Li, H. J. Zhai and Z. M. Sun, *Dalton Trans.*, 2016, **45**, 3874–3879; (d) C. C. Shu, L. Qiao, A. Muñoz-Castro and Z. M. Sun, *Chin. J. Chem.*, 2021, **39**, 1953–1957.
- F. Lips, M. Holyńska, R. Clérac, U. Linne, I. Schellenberg, R. Pöttgen, F. Weigend and S. Dehnen, *J. Am. Chem. Soc.*, 2012, **134**, 1181–1191.
- S. Mitzinger, L. Broeckaert, W. Massa, F. Weigend and S. Dehnen, *Chem. Commun.*, 2015, **51**, 3866–3869.
- S. Mitzinger, L. Broeckaert, W. Massa, F. Weigend and S. Dehnen, *Nat. Commun.*, 2016, **7**, 10480.
- F. Lips and S. Dehnen, *Angew. Chem., Int. Ed.*, 2009, **48**, 6435–6438.



- 10 F. Lips and S. Dehnen, *Angew. Chem., Int. Ed.*, 2011, **50**, 955–959.
- 11 F. Lips, R. Clérac and S. Dehnen, *J. Am. Chem. Soc.*, 2011, **133**, 14168–14171.
- 12 R. Ababei, W. Massa, K. Harms, X. Xie, F. Weigend and S. Dehnen, *Angew. Chem., Int. Ed.*, 2013, **52**, 13544–13548.
- 13 F. Lips, R. Clérac and S. Dehnen, *Angew. Chem., Int. Ed.*, 2011, **50**, 960–964.
- 14 L. Xu and S. C. Sevov, *Inorg. Chem.*, 2000, **39**, 5383–5389.
- 15 (a) S. C. Critchlow and J. D. Corbett, *Inorg. Chem.*, 1982, **21**, 3286–3290; (b) R. Ababei, J. Heine, M. Holynska, G. Thiele, B. Weinert, X. Xie, F. Weigend and S. Dehnen, *Chem. Commun.*, 2012, **48**, 11295–11297.
- 16 C. Liu, L. J. Li, X. Jin, J. E. McGrady and Z. M. Sun, *Inorg. Chem.*, 2018, **57**, 3025–3034.
- 17 B. Weinert, S. Mitzinger and S. Dehnen, *Chem.–Eur. J.*, 2018, **24**, 8470–8490.
- 18 H. von Schnering, J. Wolf, D. Weber, R. Ramirez and T. Meyer, *Angew. Chem., Int. Ed. Engl.*, 1986, **25**, 353–354.
- 19 B. W. Eichhorn, S. P. Matamanna, D. R. Gardner and J. C. Fetting, *J. Am. Chem. Soc.*, 1998, **120**, 9708–9709.
- 20 B. Kesanli, J. Fetting and B. W. Eichhorn, *J. Am. Chem. Soc.*, 2003, **125**, 7367–7376.
- 21 B. Kesanli, J. Fetting, B. Scott and B. W. Eichhorn, *Inorg. Chem.*, 2004, **43**, 3840–3846.
- 22 J. Li and K. C. Wu, *Inorg. Chem.*, 2000, **39**, 1538–1544.
- 23 W. Q. Zhang, H. W. T. Morgan, C. C. Shu, J. E. McGrady and Z. M. Sun, *Inorg. Chem.*, 2022, **61**, 4421–4427.
- 24 (a) C. E. Belin, *J. Am. Chem. Soc.*, 1980, **102**, 6036–6040; (b) M. Piesch, S. Reichl, M. Seidl, G. Balázs and M. Scheer, *Angew. Chem., Int. Ed.*, 2021, **60**, 15101–15108; (c) S. Mandal, A. C. Reber, M. Qian, R. Liu, H. M. Saavedra, S. Sen, P. S. Weiss, S. N. Khanna and A. Sen, *Dalton Trans.*, 2012, **41**, 12365–12377; (d) M. J. Moses, J. Fetting and B. W. Eichhorn, *J. Am. Chem. Soc.*, 2002, **124**, 5944–5945; (e) C. Schwarzmaier, A. Y. Timoshkin, G. Balázs and M. Scheer, *Angew. Chem., Int. Ed.*, 2014, **53**, 9077–9081.
- 25 Y. Wang, P. Zavalij and B. W. Eichhorn, *Chem. Commun.*, 2017, **53**, 11600–11602.
- 26 M. Kaas and N. Korber, *Z. Anorg. Allg. Chem.*, 2017, **643**, 1331–1334.
- 27 C. Knapp, B. Zhou, M. S. Denning, N. H. Rees and J. M. Goicoechea, *Dalton Trans.*, 2010, **39**, 426–436.
- 28 P. H. M. Budzelaar, K. H. D. Haan, J. Boersma, G. J. M. Van der Kerk and A. L. Spek, *Organometallics*, 1984, **3**, 156–159.
- 29 P. H. M. Budzelaar, A. A. H. Van der Zeijden, J. Boersma, G. J. M. Van der Kerk, A. L. Spek and A. J. M. Duisenberg, *Organometallics*, 1984, **3**, 159–163.
- 30 Z. Zhu, R. J. Wright, M. M. Olmstead, E. Rivard, M. Brynda and P. P. Power, *Angew. Chem., Int. Ed.*, 2006, **45**, 5807–5810.
- 31 (a) A. Ugrinov and S. C. Sevov, *J. Am. Chem. Soc.*, 2003, **125**, 14059–14064; (b) B. Zhou, M. S. Denning, C. Jones and J. M. Goicoechea, *Dalton Trans.*, 2009, 1571–1578; (c) S. C. Sevov and J. M. Goicoechea, *Organometallics*, 2006, **25**, 5678–5692; (d) J. M. Goicoechea and S. C. Sevov, *Organometallics*, 2006, **25**, 4530–4536.
- 32 (a) G. te Velde, F. M. Bickelhaupt, E. J. Baerends, C. Fonseca Guerra, S. J. A. van Gisbergen, J. G. Snijders and T. Ziegler, *J. Comput. Chem.*, 2001, **22**, 931–967; (b) *AMS2021, SCM, Theoretical Chemistry*, Vrije Universiteit, Amsterdam, The Netherlands, <https://www.scm.com>.
- 33 (a) J. P. Perdew, K. Burke and M. Ernzerhof, *Phys. Rev. Lett.*, 1996, **77**, 3865–3868; (b) J. P. Perdew, K. Burke and M. Ernzerhof, *Phys. Rev. Lett.*, 1997, **78**, 1396.
- 34 S. Mitzinger, L. Broeckaert, W. Massa, F. Weigend and S. Dehnen, *Nat. Commun.*, 2016, **7**, 10480.

